THE ASTRONOMICAL JOURNAL, 119:1339–1344, 2000 March

THE EVOLVING MORPHOLOGY OF THE BIPOLAR NEBULA M2-9

SEAN DOYLE[1] AND BRUCE BALICK[2]
Department of Astronomy, University of Washington, Box 351580, Seattle, WA 98195
R. L. M. CORRADI[3]
Instituto de Astrofísica de Canarias, Calle Vía Láctea, E-38200 La Laguna, Tenerife, Spain
AND
H. E. SCHWARZ[4]
Nordic Optical Telescope, Apdo. 321, E-38780 Santa Cruz de la Palma, Spain
Received 1999 October 6; accepted 1999 December 3

ABSTRACT

The planetary nebula M2-9 has drastically changed its shape since its discovery by Minkwoski. Although the outline of the nebula seems to be stationary, most of the knots and bright features (N1, N2, S1, and S2) have moved laterally from the west to the east edges of both lobes. These features and their changes have reflection, not point, symmetry. We have compiled high-quality CCD images in Hα and [O III] obtained every 2–5 years since 1985 to monitor position and morphological changes in the individual knots. Our results show that the recent structural changes are more complex than suggested previously. The pattern of changes resemble a rotating corkscrew-like pattern, as if a precessing ionization/excitation beam inscribes the knots and filaments on the pencil-shaped lobe edges. The beam flow speed is no higher than $0.01c$, so the beam is not a light beam. Its rotation period is about 120 yr. The corkscrew pattern and its apparent speed render many simple models implausible. The model of beads sliding along a helical wire is easily ruled out by observations. A model that may work is a combination of a beam and a spray of energetic particles, both invisible and moving radially at about 1000 km s^{-1}, which shock-heats and ionizes the walls of the lobes as the beams precess.

Key words: planetary nebulae: general — planetary nebulae: individual (M2-9) — stars: winds, outflows

1. INTRODUCTION

The "Butterfly" planetary nebula M2-9 (PN 10.8+18.0) was discovered and named by Minkwoski (1947). The lobes of M2-9 are cigar-shaped and oriented nearly north-south. Early studies of the nebula's morphology were made by Allen & Swings (1972, hereafter AS72), van den Bergh (1974), and Kohoutek & Surdej (1980, hereafter KS80), all of whom noted the changes in the structure of M2-9 since Minkowski's first image. The best reproductions of these early photographs are found in Aller & Liller (1968) and AS72.

These studies were based on photographic images of M2-9 made using a variety of poorly characterized filters. Even so, the changes in the structure of M2-9, in which the brightest features appear to move from west to east laterally across its lobes, were obvious. As Figure 1 shows, by the 1980s the nebula was almost a mirror image of its 1952 appearance. AS72 and van den Bergh (1974) proposed that the changes were the result of a rotating beam of ionizing radiation from the star shining through a matched pair of holes in orbiting dust clouds. Alternatively, KS80 suggested that the nebula was rotating as a whole. Goodrich (1991) and Trammell, Goodrich, & Dinerstein (1995, hereafter TGD) suggested that a rotating north-south fan beam of ionizing emission sweeps through the lobes, producing bright "moving" knots of gas where it intersects high-density rings or sheaths that gird the lobes' edges.

Images obtained in the 1980s and early 1990s showed that the trends of west-to-east motions continued (cf. Hora & Latter 1994, hereafter HL94). Goodrich (1991) realized that if the motions were the result of a precessing beam of ionization the moving features should leave a trailing recombination tail in their wake. However, TGD could not find this tail. TGD also argued against solid-body rotation. They noted that such rotation requires excessively large matter velocities (of order 10^3 km s^{-1}) if M2-9 is at its preferred distance and that there should be concomitant Doppler-shift gradients that are not seen (e.g., Icke, Preston, & Balick 1989).

We have compiled digital copies of images taken ever since CCD detectors on high-quality telescopes have been used to image M2-9. Although the quality of both the seeing and the detectors differs from one image to another, the results are clear: the changes continue. However, the bright features nearest the star have begun to move back toward the west, while others beyond about 10″ from the nucleus continue their eastward course. In this paper we briefly discuss the sources of the images, describe the morphological changes that have occurred in the past 14 years, and speculate on the mechanism(s) that cause the changes.

In all figures, north is to the top and east is to the left. We follow the standard feature identification nomenclature for M2-9 of KS80 and HL94.

2. DATA AND RESULTS

Images from several different observers, telescopes, and conditions were used in this study (Table 1). Some of these images have appeared elsewhere, e.g., Balick (1987), Schwarz, Corradi, & Melnick (1993), and Schwarz et al. (1997, hereafter SACR), whereas others are unpublished. As

[1] smdoyle@u.washington.edu.
[2] balick@astro.washington.edu.
[3] rcorradi@ing.iac.es.
[4] hschwarz@not.iac.es.

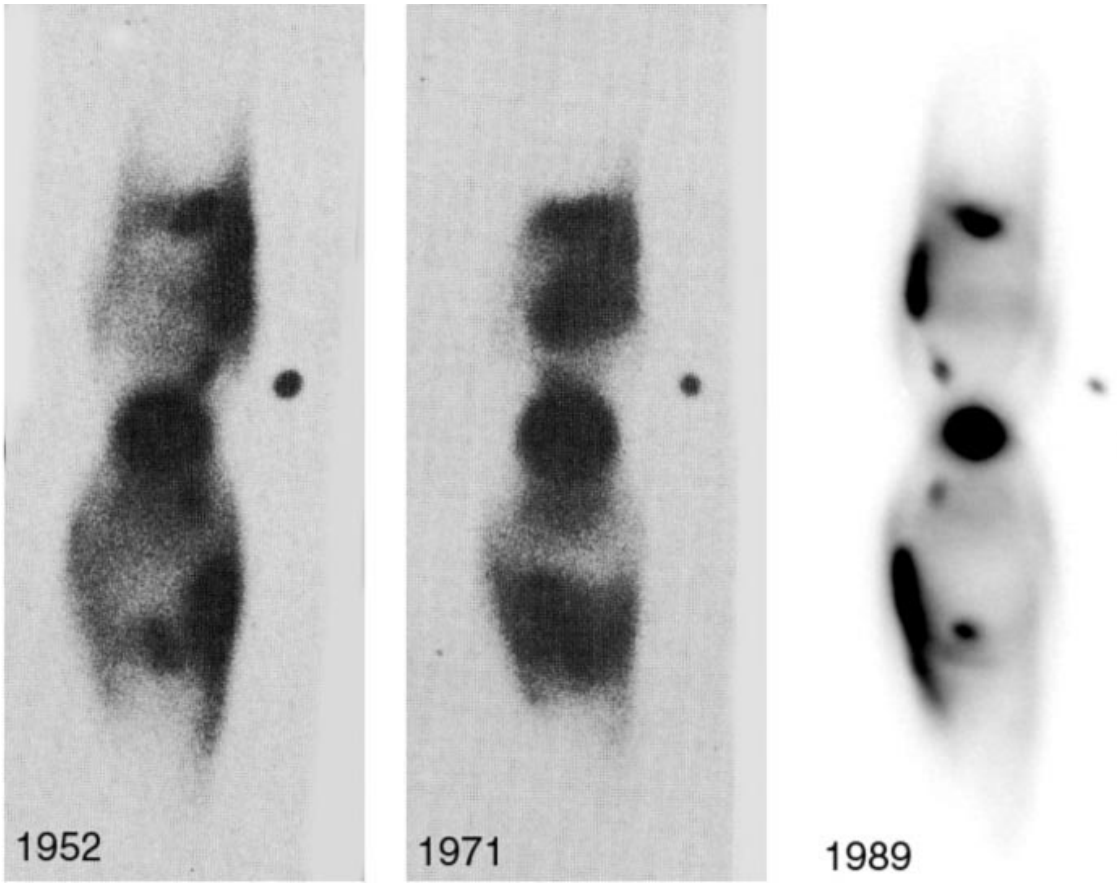

FIG. 1.—Images of M2-9 spaced by approximately 19 yr. North is to the top and east is to the left. Note the changes in structure, primarily from west to east. The 1952 and 1971 photographs are reproduced from AS72. The 1989 CCD image is described in Table 1.

a test of the fidelity of the ground-based images, we convolved *Hubble Space Telescope* (*HST*) images obtained in 1997 by Balick, Mellema, & Icke (2000, hereafter BMI) to match the seeing conditions of ground-based observations made at about the same time. These sets of images agree extremely well.

For display purposes, the intensities of the images were scaled to the flux through an aperture that includes only the stationary knot N3 (however, we have no evidence that the flux of this knot is constant). Two series of images, one from nine Hα filter images and the other from five deep [O III] images, were aligned to a common orientation, center, and magnification and then stacked into two animations. Some of the Hα images were obtained through filters that include the [N II] λ6583 line in the bandpass; however, *HST* images by BMI in Hα and [N II] show that M2-9 looks almost indistinguishable in both lines.

TABLE 1

M2-9 IMAGE CHARACTERISTICS

Epoch	Telescope	Filter	Exposure (s)	Seeing[a] (arcsec)
1985.9	Kitt Peak 2.1 m TI2	Hα	60	2.9
1985.9	Kitt Peak 2.1 m TI2	[O III]	600	2.2
1988.5	2.2 m ESO + Adapter	Hα	...	1.4
1989.4	NTT + EFOSC2	Hα	120	0.9
1989.4	NTT + EFOSC2	[O III]	120	0.5
1991.6	NTT + EMMI	Hα	60	0.8
1993.3	3.6 m ESO + EFOSC	Hα	20	1.4
1994.5	3.6 m ESO + EFOSC	Hα	180	1.5
1996.6	NOT + BROCAMII	[O III]	180	0.7
1997.6	NOT + ALFOSC	Hα	20	0.7
1997.7	*HST* WFPC2	Hα	1200	[0.7]
1997.7	*HST* WFPC2	[O III]	1000	[0.7]
1999.75.....	NOT + ALFOSC	[O III]	300	0.7
1999.8	NOT + Hirac II	Hα	240	0.9

[a] Values in brackets are the result of digital deconvolution.

The most conspicuous changes in the morphology are the lateral motions of the knots N1, N2, S1, and S2. These changes are illustrated in Figure 2*c*, using two-color overlays of pairs of high-quality images obtained in 1989 and 1999. Also shown in Figure 2*c* is an overlay of the Hα and [O III] images from the *HST* obtained in 1997.7, which gives a 0.″1 resolution "snapshot" of M2-9 at one epoch.

Interestingly, although N1 and S1 had moved from the west to the east edges of their respective lobes by 1994 (HL94), we find that they subsequently reversed the sense of their motion. By 1996 both N1 and S1 had developed a comet-like shape, with the heads seen best on [O III] images. Comae and east-pointing tails are conspicuous in the Hα, [N II], [S II], and [O I] images obtained with the *HST* in 1997.7 (BMI) and confirmed by subsequent ground-based images.

Filaments N2 and S2 have likewise laterally traversed the nebula from west to east between 1952 and the 1980s. Since then, they have generally remained near the east edges of the two bipolar lobes. However, the shapes of N2 and S2

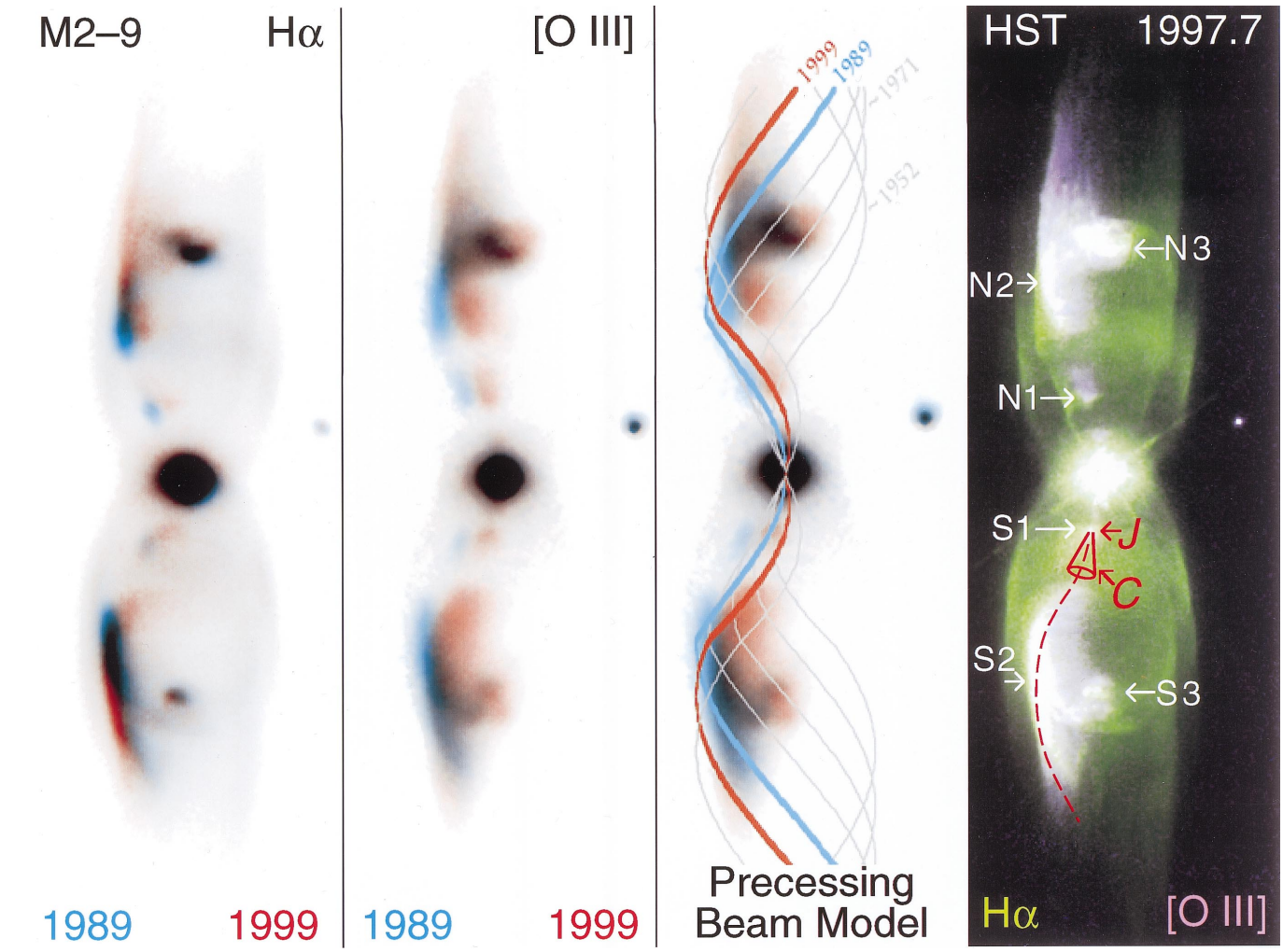

FIG. 2.—Figs. 2*a* and 2*b* appear in the electronic edition of The Astronomical Journal. Fig. 2*c* shows various overlays of image pairs of M2-9, each chosen selectively from the images of Fig. 1. *Left*: Hα images obtained in 1989 (*cyan*) and 1999 (*red*) under conditions of excellent seeing. These show the morphological evolution of the nebula. *Second*: [O III] images obtained in 1989 (*cyan*) and 1999 (*red*) under conditions of excellent seeing. *Third*: Using the previous panel as background, we show a heuristic corkscrew model, which is fitted by eye to the [O III] morphologies seen in 1989 and 1999. Each line is a model in which the projected corkscrew turns by 30°. *Right*: Unconvolved *HST* Wide Field Planetary Camera 2 images from 1997.7 in Hα (*green*) and [O III] (*magenta*). A red "J" marks the point where the southern jet contacts the outer lobe, forming a bright [O III] knot. The cone marked "C" indicates the spray pattern emanating from J.

have evolved continuously since 1985. The star-facing (inner) ends of these filaments follow the motions of N1 and S1 from east to west, suggesting that, in spite of obvious gaps that separate N1 from N2 and S1 from S2, there exists a physical connection between the knots and filaments. On the other hand, the outer regions of N2 and S2 continue to move from west to east. The centers of the filaments have moved only slightly. Also, long north-south extensions to the lobes have become apparent in the Hα images, though this may be an artifact of the ever-improving sensitivity of CCDs.

Meanwhile knots N3 and S3 have not moved. There are hints that they may have expanded at times, but the location of their peak intensities seems to be nearly fixed. They seem to be knots located near the lobes' axes of symmetry.

3. DISCUSSION

M2-9 lies at a distance of 640 ± 100 pc and is oriented almost face-on, between 11° and 15° from the plane of the sky (SACR; Goodrich 1991). Observers who have mapped the Doppler shifts of the lobes (Balick 1989; SACR; BMI) all find that the gas streams outward through the lobes at 100 km s^{-1} or more beyond about 4″ of the nucleus.

The pattern of features and changes in the positions of the knots and filaments in M2-9 has constantly maintained reflection, or mirror, symmetry about both of its cardinal axes, not point symmetry through its nucleus. This symmetry is unusual among planetary nebulae, for example, SS 433. All featured motions seem to be almost entirely lateral; i.e., there is little if any direct evidence of radial (outstreaming) motions. This is somewhat surprising in view of the common expectation that collimated gas flows outward through the narrow lobes of bipolars.

The motions of N1, S1, N2, and S2 suggest that all of these moving features are inscribed on the surfaces of the lobes' walls and not the lobes' interiors. This would be characteristic of illumination-excitation effects on the lobe walls. The illuminating beam, whether composed of photons (AS72; van den Bergh 1974) or particles, is not directly observable. Only its effects on the walls are visible.

Unlike the N1-S1 and N2-S2 feature pairs, the N3-S3 features have no apparent secular motions, though some scatter in their locations is allowed by the present data (see also KS80 and HL94 for a summary of the historical astrometry). N3 and S3 certainly do not exhibit the pattern changes that affect the other knots, perhaps because they lie on the nebular symmetry axis or because they arise from, say, stationary shocks where gas flows converge. This is plausible because the outermost, very faint lobes of M2-9 (SACR) have high outflow velocities and are probably pushed by a supersonic and thus invisible wind coming from the central object. Note that the velocities of the (reflected) light in N3 and S3 Hα and [N II] lines show a 40 km s^{-1} difference, making it likely that the light for [N II] comes from N3 and S3, while that of the Hα line comes from the central region (SACR). We do not discuss N3 and S3 hereafter. See BMI for more details.

Ignoring all physics, we propose a geometric model that accounts for the changing morphology of M2-9. The pattern of moving features resembles a pair of right- and left-handed corkscrews or springs joined at the nucleus. The corkscrew rotates with a period of about 120 yr, close to that estimated by AS72.

This rotating corkscrew pattern is inscribed on the walls of the pencil-shaped lobes. The corkscrew turns by 90° out to the inflection point of the pencil. Thereafter, the spiral pattern continues with the same period along the walls of a cylinder. The fit of the model to the [O III] image is shown in Figure 2*c*.

The model fit is only fair. Nonetheless, it matches the historical changes of the nebula far better than does a pair of revolving searchlights. The pencil-corkscrew model accounts nicely for the locations and motions of knots N1 and S1 and the inner portions of N2 and S2, which are presently moving in one direction, and the outer parts of the filaments, which are moving in the other.

Tails seen in Hα, [N II], [S II], and [O I] trail behind knots N1 and S1 and the inner portions of filaments N2 and S2 (BMI; see also Fig. 2*c*, *right*). These tails move nearly synchronously, with a slight lag behind the corresponding nearest [O III] features. Presently, the tails stretch eastward from N1, S1, and the lower portions of N2 and S2, not westward, where TGD looked for them. (From 1990 to 1995, projection effects would have rendered the tails unresolvable in the apertures that TGD used for their spectroscopic observations.) The east-west orientation of these tails is consistent with the hypothesis that the features move laterally.

Some scattered light is clearly present in the M2-9 nebula: polarization levels are in the range 10%–20% in the inner features and 60% in the outer, faint lobes (King et al. 1981; SACR). So not all light is due to local emission; some comes from the central source and is scattered or reflected. TGD found that the degree of the polarization in emission lines from the knots is less than in their immediate surroundings. This argues that much of the knot emission is largely intrinsic, whereas line emission arising elsewhere in the lobes contains intrinsic and scattered components.

4. INTERPRETATION

4.1. *Implausible Models*

How can the lateral motions of features of M2-9 be explained? One class of models is that of the bulk motions of luminous knots. The simplest, but completely ad hoc explanation, is that of rotation of a helical pattern of knots inscribed on a cylinder rotating about the nebula's axis of symmetry (AS72). However, the observed proper motions require a velocity of 10^3 (D/640 pc) km s^{-1}, where D is the distance to M2-9, but this is easily ruled out by observations of Doppler shifts of the knots as they reach the cylindrical edge (BMI).

Another class of explanations is that of bulk motions of luminous knots ejected by a precessing nozzle. A variation of this is the model of "beads" sliding along twisted "wires" attached to a rotating star. Both types of models are easily eliminated since no outward proper motions of any knots are observed.

To be more quantitative, the moving features of M2-9 exhibit only modest Doppler shifts. After correction for projection, their flow velocities are of order 50–100 km s^{-1} (e.g., AS72; Carsenty & Solf 1983; Icke et al. 1989) and not higher than 170 km s^{-1} (SACR). However, the velocity of the corkscrew pattern propagation is about 30″ or about $10^{12.5}$ km in about 100 yr (about $10^{9.5}$ s) or about 1000 km s^{-1}. Hence, the pattern velocity in M2-9 is higher than that of the bulk motions of the pairs N1-S1 and N2-S2 by an order of magnitude.

Several authors have proposed a rotating beam of photon excitation. This ad hoc suggestion was based on the assumption that the moving knots are located at a single azimuth from the star, so that a rotating fan beam of ionizing and heating stellar light from the star will cause a changing illumination pattern. The polarization data support local ionization and heating (by ultraviolet light or shocks) since the fractional polarization is lowest in the moving knots.

The corkscrew pattern of moving knots complicates this model, but does not necessarily falsify it. At the measured distance of M2-9, 640 pc, the light travel time radially through the about 30″ lobes is only a few months. Therefore, a simple rotating illumination fan beam model can be eliminated since it cannot produce a helical pattern of moving knots. Instead, the observed pattern of knot pairs, N1-S1, N2-S2, and N3-S3, requires two carefully matched ultraviolet illumination patterns of the same peculiar shape, one each for the N and S lobes. This is extremely implausible.

In summary, beamed ultraviolet illumination models seem highly unlikely. Bulk motions of knots are eliminated as explanations for the evolving morphology of M2-9. A realistic physical model must be more complex than either of these.

4.2. *A Particle (Fluid) Jet-Splash Model*

A variation of a fluid beam model can be contrived to explain the observations. We propose a model in which the high-speed motions are ultimately powered by a pair of nonradiative collimated particle beams ("jets") characterized by a speed in excess of 1000 km s^{-1} (see discussion below). These invisible jets are ejected from the nucleus through nozzles with a rotation period of about 120 yr.

Shocked line emission forms at the working surfaces where the jets encounter the dense lobe edges. These working surfaces are seen as the bright knots on the star-facing side of N1 and S1 in the [O III] image of Figure 2*c* (labeled "J"). Owing to the orientation of M2-9 near the plane of the sky, the observed loci of impact points of the

two beams degenerate into two parallel lines, so the apparent motions of N1 and S1 are lateral.

The normal component of each jet's momentum is converted into heat at the working surface, which is partially converted into escaping line emission. The obliquity of the impact apparently produces shocks driven into the walls at speeds $\lesssim 150$ km s^{-1}, or else the [O III] lines would not be bright. It is important to note that the observed Doppler shifts are primarily those of the gas in the lobe walls and not the jets.

The glancing jet-wall interaction produces a cone of spray downstream from each splash point (labeled "C" in Fig. 2*c*). Like the jet, the spray is invisible. The transverse component of the momentum of the fluid beam is transferred to the released spray. We shall suppose that the spray includes additional mass from the lobe walls. Accordingly, the speed of the spray propagation is somewhat less than that of the original beam.

Extended emission appears where the spray cone intersects, ionizes, and shocks the lobe walls downstream. The intersection of the cone and the lobe edges north of the nucleus is seen in the [O III] image of Figure 2*c* as the combination of a northward "stub" on N1 plus all of N2. The southern counterpart of the cone-wall intersection is the mirror image of its northern counterpart. Odd gaps between N1 and N2 and between S1 and S2 arise where the spray cone fails to make contact with the lobe walls because of the local geometry of the latter.

The combination of jet rotation and spray propagation inscribes an apparent spiral pattern of excitation on each of the lobes' walls. It is the speed of the invisible spray, apparently about 1000 km s^{-1}, that accounts for the apparent outward motion of the corkscrew pattern since 1952.

The most highly ionized material in the lobe walls recombines as the jet splash point and its spray cone move onward. This forms the trailing recombination regions seen in Hα, [N II], and [S II] behind N1, N2, S1, and S2, as predicted by Goodrich. Obviously the O^{++} recombination time, $\tau_{O^{++}} \lesssim 10$ yr, is shorter than the recombination time of H^+, N^+, and O^+ by an order of magnitude, because of the ratio of their recombination coefficients. The implied electron density in the O^{++} zone and the lagging recombination tails is 10^4 yr$/\tau_{O^{++}} \gtrsim 10^3$ cm^{-3}. (Presumably H^+, N^+, and O^+ do not recombine completely because of stellar photoionization.)

The density at the lobe walls is important since the combination of jet-spray ram pressure and ablation might erode or destroy low-density working surfaces. TGD obtained detailed spectra in N2 and S2 and regions immediately to the west. In S2 and N2, the [S II] diagnostic line ratio was in the upper density limit (electron density $n_e \gtrsim 10^4$ cm^{-3}). Farther west, n_e drops to about 10^4; BMI find that the [S II]/[N II] ratio measured from narrowband images decreases where the surface brightness is highest in the lobes, suggesting that the [S II] lines are partially quenched and confirming that the densities are high. No observations of densities have been made at N1 and S1. BMI find that the [S II] line is unobservable at N1 and S1, the result of either ionization stratification or very high densities.

In short, these rough estimates of the density distribution suggest that the spray (and presumably the jet) compresses the lobe walls and enhances their emission measures. Apparently the walls "rebound." Driven by their internal thermal pressure, the walls expand at their sound speed and recover their initial density within a decade or two as the spray interaction zone moves elsewhere. The wall thickness is thus of order 10^{15} cm, or about 1 pixel in the *HST* image.

The speed of the jets that strike N1 and S1 is another key parameter for this model. The beam speed can be estimated from the outflow-broadened circumnuclear Hα line (Balick 1989; Torres-Peimbert & Arrieta 1997). The wings of this line extend beyond 5000 km s^{-1}. Consequently we shall adopt a beam speed $\gtrsim 0.01$ *c*, or perhaps slightly higher. The exact speed is not important for this conceptual model.

This physical concept of wind- (or beam-) lobe interactions for steady isotropic winds interacting with lobe walls was developed by Cantò, Tenorio-Tagle, & Różyczka (1988) in the context of Herbig-Haro (H-H) objects. Frank, Balick, & Livio (1996) applied the same concept to planetary nebulae. See these papers for a discussion of the physics. Also, see BMI for a more detailed observational description of M2-9.

No matter what the nature of the beam, it will etch and erode the walls of the lobes in time through ablation. At the same time, the splash points should eventually grow into protuberances. To say any more would be wild conjecture. Nonetheless, a study of the shape, mass distribution, and dynamical stiffness of the material outside the walls would be a very useful step. Its possible that magnetic fields are required to maintain the geometry of the lobe walls against the cumulative bombardment impacts of the precessing jets. Such fields at the lobe perimeter may have been swept and compressed by stellar winds (e.g., Chevalier & Luo 1994).

4.3. *Forming Collimated Particle Beams*

What forms the collimated particle beam? One possibility is that mass lost from the surface of an asymptotic giant branch star (like a Mira) in a binary system produces strong density gradients, along the binary axis of the circumstellar gas/dust. A two-sided collimated outflow from a hot, compact companion might be deflected in the direction opposite to the red giant by these density gradients. This would account for the mirror symmetry of the features of M2-9, whose rotational period would then be related to the orbital period of the system. The emerging gas flow should be a pair of beams with a wide-angle V-shaped geometry.

The apparent corkscrew rotation period, which lies between 100 and 150 yr, is a timescale more typical of orbital periods (or stellar/disk precession) rather than of stellar rotation. It is consistent with the orbital periods of symbiotic Miras with an orbital separation of about 30 AU. The binary system would be detached at this orbital radius with no Roche lobe overflow. It is not fully clear, even for symbiotic stars, if at such separations the interaction between the two stars can be very effective at forming highly collimated fluid beams.

Certainly, the star with the extended atmosphere would have to be a very extended post–red giant. The spectrum of the central star of M2-9 supports this sort of an interpretation. It has an odd emission-line spectrum, rich in Fe II lines, but one that is similar to that of a symbiotic (AS72; Balick 1989).

Many of the nebulae around classical symbiotics, such as He 2-147, HM Sge, and V1016 Cyg (Corradi et al. 1999), are associated with highly bipolar nebulosities. Such symbiotics can produce complex, variable winds as a combination of ionizing radiation and fast winds from a hot companion interacts with the slower, massive winds from a Mira-like

primary, perhaps producing strongly shocked, eruptive, precessing, organized patterns of winds. M2-9 may presently be observed in a propitiously active stage of mass loss.

Another example may be the case of He 2-104 (Schwarz, Aspin, & Lutz 1989), which has a Mira and has HH-like objects flowing away at about 100 km s^{-1}, probably pushed by some invisible beam that, given the geometry, must be highly collimated (rough estimate: aspect ratio is 10 or more). So at least one Mira-containing symbiotic is reminiscent of the odd behavior pattern of M2-9.

The changing morphology of M2-9 provides new insight into the evolution of mass ejection into bipolar nebulae. We intend to continue an imaging program in space and on the ground in the years ahead. Anyone who obtains a good image of M2-9 is encouraged to contact one of us.

The suggestions of an anonymous referee were extremely helpful in motivating the physical model presented in § 4.2. B. B. is very grateful for support provided by NASA through grant GO 6502 from the Space Telescope Science Institute, which is operated by the Association for Research in Astronomy, Inc., under NASA contract NAS 5-26555, and research grant AST 94-17112 from the National Science Foundation.

REFERENCES

Allen, D. A., & Swings, J. P. 1972, ApJ, 174, 583 (AS72)
Aller, L. H., & Liller, W. 1968, in Nebular and Interstellar Matter, ed. B. M. Middlehurst & L. H. Aller (Chicago: Univ. Chicago Press), 483
Balick, B. 1987, AJ, 94, 671
———. 1989, AJ, 97, 476
Balick, B., Mellema, G., & Icke, V. 2000, in preparation (BMI)
Cantò, J., Tenorio-Tagle, G., & Różyczka, M. 1988, A&A, 192, 287
Carsenty, U., & Solf, J. 1983, in IAU Symp. 103, Planetary Nebulae, ed. D. R. Flower (Dordrecht: Reidel), 510
Chevalier, R. A., & Luo, D. 1994, ApJ, 421, 225
Corradi, R. L. M., Ferrer, O. E., Schwarz, H. E., Brandi, E., & Garcìa, L. 1999, A&A, 348, 978
Frank, A., Balick, B., & Livio, M. 1996, ApJ, 471, L53
Goodrich, R. W. 1991, ApJ, 366, 163
Hora, J. L., & Latter, W. B. 1994, ApJ, 437, 281 (HL94)
Icke, V., Preston, H. P., & Balick, B. 1989, AJ, 97, 462
King, D. J., Perkins, H. G., Scarrott, S. M., & Taylor, K. N. R. 1981, MNRAS, 196, 45
Kohoutek, K., & Surdej, J. 1980, A&A, 85, 161 (KS80)
Minkowski, R. 1947, PASP, 59, 237
Schwarz, H. E., Aspin, C., Corradi, R. L. M., & Reipurth, B. 1997, A&A, 319, 267 (SACR)
Schwarz, H. E., Aspin, C., & Lutz, J. 1989, ApJ, 344, L29
Schwarz, H. E., Corradi, R. L. M., & Melnick, J. 1993, A&AS, 96, 23
Torres-Peimbert, S., & Arrieta, A. 1997, Rev. Mexicana Astron. Astrofis., 7, 171
Trammell, S. R., Goodrich, R. W., & Dinerstein, H. L. 1995, ApJ, 453, 761 (TGD)
van den Bergh, S. 1974, A&A, 32, 351